EQUINE VETERINARY JOURNAL

EQUINE VETERINARY JOURNAL
Equine vet. J. (2010) **42** (Suppl. 38) 475-481
doi: 10.1111/j.2042-3306.2010.00221.x

Heel effects on joint contact force components in the equine digit: a sensitivity analysis

P. NOBLE*, **J.-P. LEJEUNE**[†], **I. CAUDRON**[†], **P. LEJEUNE**[†], **B. COLLIN**, **J.-M. DENOIX**[‡] and **D. SERTEYN**[†§]

Division of Anatomy, Department of Morphology and Pathology, Faculty of Veterinary Medicine, Liège University, Belgium; [†]Centre Européen du cheval, Mont-le-Soie, 1, Vielsalm, Belgium; [‡]Centre d'imagerie et de recherche en affection locomotrice equine (CIRALE), Dozulé, France; and [§]Division of equine clinic, Department of Clinical Science, Liège University, Belgium.

Keywords: horse; inverse dynamic analysis; trot; wrapping force; joint contact force

Summary

Reasons for performing study: **Whereas the effect of heel configuration on the tension of the suspensory apparatus is well documented in the literature, there are few reports of joint contact force components in the equine distal forelimb.**

Objectives: **To improve understanding of the effect of heel configuration on equine digit joint loading, a sensitivity analysis was performed to compare the effect of a raised heel on joint contact force components in the coffin and fetlock joints during the stance phase of the trot.**

Materials and methods: **Four Warmblood horses were used. An inverse dynamic analysis was carried out using kinematic and kinetic data. Taking into account the tendon wrapping forces (WF) around the sesamoid bones in the calculations, the joint contact forces (CF) were estimated for the coffin and fetlock joints during the trot stance phase (4 m/s). To test the sensitivity of the results to heel configuration changes, calculations were performed repeatedly for different heel configurations (raised by 0, 6 and 12°). A one-way ANOVA with repeated measures was used to test the effect of heel configuration (at the 3 levels) ($\alpha = 0.05$; P<0.05; *post hoc* testing: Bonferroni).**

Results: **For heel configurations raised from 0–12°: whereas the tension of the deep digital flexor tendon decreased and the tension of the superficial digital flexor tendon increased, for the coffin joint the peak WF (1.4 ± 0.25 bwt; 1.2 ± 0.2 bwt; 0.95 ± 0.1 bwt) and the peak CF (2.45 ± 0.25 bwt; 2.2 ± 0.2 bwt; 2 ± 0.1 bwt) decreased significantly (P<0.05). For the fetlock joint, the peak WF (3.8 ± 0.7 bwt; 4.1 ± 0.3 bwt; 4.4 ± 0.25 bwt) and the peak CF (4.35 ± 0.7 bwt; 4.7 ± 0.35 bwt; 5 ± 0.3 bwt) increased, but not significantly.**

Conclusion: **This analysis suggests that the coffin joint loading and fetlock joint loading are strongly connected. The heel configuration may influence both coffin joint and fetlock joint contact force components.**

Introduction

Excessive biomechanical stresses are commonly believed to be important in the pathogenesis of various osteoarticular disorders (Radin *et al*. 1972; Radin 1983). Traditionally, external reaction forces have been used to investigate experimentally the relationship between mechanical loading and contact areas or pressure distribution. Nevertheless, external reaction force, corresponding to the sum of forces acting in opposite directions (joint contact force, muscle forces), only represents a resultant value of a subtraction. Moreover, one modelling study estimated that muscles crossing the human ankle joint contribute to an additional 7 bwt of force during running (4 m/s) (Sasimontonkul *et al*. 2007). Therefore, knowledge of joint contact force is likely to be relevant in understanding the correlation between mechanical loading and osteoarticular disorders.

Considerable research has been conducted to present a detailed model of the equine distal limb and a methodology for calculating musculotendon forces (Meershoek and Lanovaz 2001; Meershoek *et al*. 2001, 2002; Brown *et al*. 2003). However, these studies did not go as far as calculating joint contact forces. More recently, Merritt *et al*. (2008) developed a model to understand the influence of muscle-tendon wrapping on calculations of joint contact force magnitude for the coffin and the fetlock joints. To our knowledge, little work has yet been done to evaluate the potential effect of heel configuration changes on joint contact force components in the equine digit during movement.

The purpose of this study was to estimate joint contact force components in the fetlock and coffin joints during the trot stance phase, from an inverse dynamic analysis and to investigate the effect of heel configuration changes on joint contact force components from a sensitivity analysis.

Materials and methods

Collection of in vivo *data*

Four Warmblood horses were used (3 geldings and one mare). Their age ranged from 3.5–8.5 (mean 5.5) years and their body mass from 500–580 (mean 543.5) kg. None had a recent history of lameness and all were judged to be sound on clinical examination. Horses were shod with Classic Roller Steel horseshoes[1] with one radius clip ranging from size 1 to size 3.

According to the rules that respect the biomechanical balance of the foot (Caudron 1997), horses were trimmed and shod, by an

*Corresponding author email: pnoble@ulg.ac.be
[Paper received for publication 09.01.10; Accepted 13.06.10]

experienced farrier, with a nonbroken foot-pastern axis before any addition of a heel wedge.

As the study was conducted on a treadmill (Mustang 2200)[2], the horses were accustomed to walk and trot before testing took place. On the day of the tests, the horses were led at a trot of 4 m/s. Kinetic and kinematic data were collected during 3 following sessions: to both shod forehooves, before application of heel wedge, after application of 6 and 12° heel wedges[1]. For each session, data from 10 strides (kinematic) and 3 strides (kinetic) for each left forelimb of each horse were averaged. Kinematic data were collected using a 3D kinematic analyser, which was made up of 9 infrared (IR) cameras positioned around the treadmill. The capture, tracker and analyser software was the Smart Motion Capture System (Version 1.10.368.0)[3]. For each horse, 4 markers were glued on the left forelimb to identify limb segments and joint centres of rotation (Fig 1), using a similar segment identification method to the one described in published morphometric data (Buchner *et al*. 1997): 1) lateral distal hoof wall, 2) proximal hoof wall over distal phalanx 2 condyle, 3) centre metacarpal condyle, and 4) ulnar carpal bone. The positions of markers 1, 2 and 3 were marked with metallic marks and lateral radiographs of the fetlock and coffin joints were used to control their position. The 3D positions of the markers were followed using the Kinematic Elite System at a frequency of 120 Hz. At square standing and during the trot, the 3D positional data of markers were collapsed onto a sagittal plane.

Kinetic data (ground reaction force) were obtained using the F-scan system (Version 5.24)[4]. This system uses an ultra thin (0.18 mm), flexible and trimmable sensoring layer with 5 sensors per cm^2. The F-scan software offers the opportunity to visualise global vertical forces under the solar surface of the foot in real time or to record it for detailed analysis. The in-foot shoe force sensor was trimmed to the tail of each forehoof, placed between 2 very stiff soles and inserted into an Equi Boot[5] which was connected to a Compaq S710 computer loaded with the F-Scan software. The sensors were calibrated at rest on a weightbearing foot, with the opposite limb being raised. On the treadmill, the in-foot shoe sensor's information was recorded at trot (4 m/s) at a frequency of 120 Hz. In order to obtain kinetic sagittal plane information, the vertical force data were combined with horizontal force data obtained from the work of Merkens *et al*. (1993) on Warmbloods of comparable type to those in the present study. Briefly, for each horse the published mean horizontal force data, expressed in N/kg bwt for a stance phase at 4 m/s, were multiplied by the ratio of the vertical force data of the horse (obtained with the F-scan and expressed in N/kg) on the published mean vertical force data (N/kg) and multiplied by body mass of the horse. The obtained values were then combined with the individual gross vertical force to have nominative kinetic sagittal plane information.

Calculation of net joint moments

The mass, inertial moment and location of the mass centre of the hoof, pastern and metacarpal segments were determined using published regression equations (Buchner *et al*. 1997). By carrying out an inverse dynamic analysis from the segment data combined with kinetic and kinematic data, the net joint moments were obtained for the coffin and for fetlock joints.

Forelimb model

According to the forelimb pulley model described by Meershoek *et al*. (2001) and taking into consideration the fact that muscle moment arms of the deep digital flexor (DDF) *(M. flexordigitorum profundus)* and superficial digital flexor (SDF) tendons *(M. flexor digitorum superficialis)* in the fetlock joint cannot be modelled as fixed-radius pulleys (Brown *et al*. 2003), a modified 2D sagittal plane forelimb model with variable-radius pulleys for the DDF and SDF tendons was considered (Fig 2). Briefly, in order to quantify the variable-radius pulley parameters (Fig 3), 11 forelimbs, from Warmbloods of comparable weight to those in the present study, were collected, transversally cut below the shoulder joint, frozen and cut into a sagittal plane as far as just above the fetlock joint. Following the segment based coordinate system described by Meershoek *et al*. (2001) for the fetlock joint, the pulley centres of the DDF and SDF tendons, the joint centre and segment axis were determined directly from the section. For the fetlock radius-pulley experiments, forelimbs were thawed overnight, fixed to an immobilising support and attached to a hoist, which extended the fetlock joint in determined angles. For the fetlock dorsal angle (θ) of 180–150°, the radius pulleys of the DDF and of the SDF tendons were measured directly from the section. For each tendon, all these data were fitted using a polynomial regression model and the relationships between θ and the variable-radius pulleys were described assuming that the radius pulley delta (Δd) was zero at a fetlock dorsal angle of 180°:

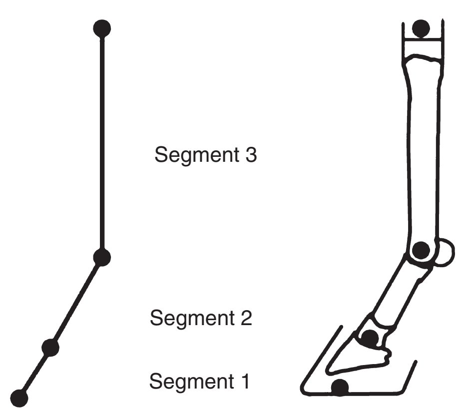

Fig 1: Placement of skin markers relative to underlying bony landmarks (right), markers used to identify limb segments and rotation centres of the joints (left).

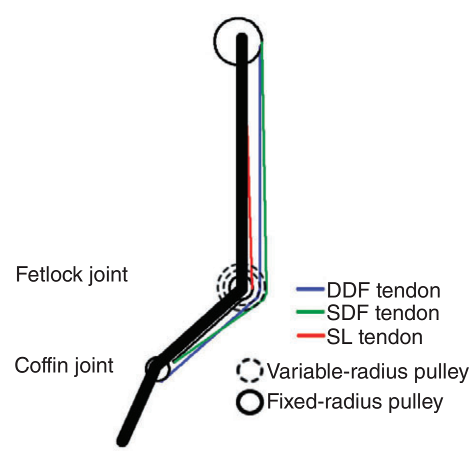

Fig 2: Two-dimensional, sagittal plane model of the equine digit (the model contains 3 rigid segments and 3 major tendinous structures).

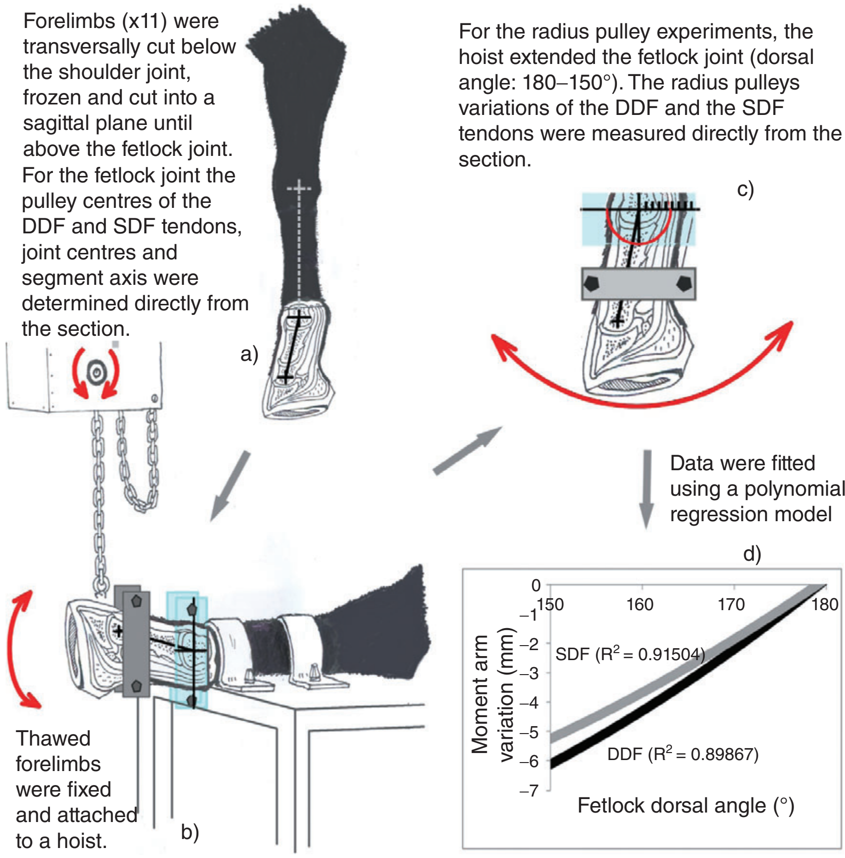

Fig 3: Fetlock radius-pulley experiments: forelimb preparation (a); forelimb fixation (b); radius-pulley experiment (c); data fitting (d).

$\Delta d_{DDF}(\theta) = -0.24923 \times \theta^1 + 0.00139 \times \theta^2$ ($R^2 = 0.89867$) for the DDF tendon and $\Delta d_{SDF}(\theta) = -0.21494 \times \theta^1 + 0.0012 \times \theta^2$ ($R^2 = 0.91504$) for the SDF tendon. This model was validated by means of direct measurements.

In the present study, for each horse, the left digit was radiographed using a mobile x-ray machine (Gierth RHF 200ML)[6] and phosphor plates (cephalometric 20 × 30 cm). Metallic marks were placed on each left digit, in order to identify the position of the DDF and SDF tendons. Following the segment-based coordinate system described by Meershoek *et al.* (2001), θ and the radius pulleys of the DDF (d^{RX}_{DDF}) and SDF (d^{RX}_{SDF}) tendons were directly measured from the radiographs. For the trot stance phase of each horse, the variable-radius pulleys of the DDF tendon and of the SDF tendon were calculated using the previous experimental θ- radius pulley relationships: $d_{SDF}(\theta) = d^{RX}_{SDF} - \Delta d^{RX}_{SDF} + \Delta d_{SDF}(\theta)$ and $d_{DDF}(\theta) = d^{RX}_{DDF} - \Delta d^{RX}_{DDF} + \Delta d_{DDF}(\theta)$.

Tendon tension and joint contact force calculations

The forelimb model was used to calculate the tensions in SDF, DDF tendons and suspensory ligament (SL), as well as the joint contact forces at the coffin and the fetlock joints.

The tension of the DDF tendon was calculated by balancing the joint moment (M) at the coffin joint with the moment arm. The tension of the SL was calculated using a method proposed by Meershoek *et al.* (2001). The strain of the SL, ($\varepsilon(t)$, was first calculated assuming that it was zero at an angle of the fetlock joint equal to the joint angle at the start of the stance phase. The tension of the SL was finally deduced using an experimentally-derived strain-force relationship (Meershoek *et al.* 2001). The tension of the SDF tendon was then deduced after subtracting the moments exerted about the fetlock joint by both the SL and the DDF tendon.

Considering the wrapping forces (WF), exerted by the sesamoid bones on the middle phalanx and on the distal metacarpus, as part of the calculation of the joint contact forces (CF), CF were calculated at the coffin and fetlock joints by enforcing equilibrium of all forces acting on the segments.

Sensitivity analysis

In order to test the sensitivity of the results to heel configuration changes, for each horse kinematic and kinetic data were collected for 3 heel configurations (0, 6 raised, 12° raised). For each session the tension of the DDF, SDF and SL tendons, the WF norm and CF norm were calculated. The obtained results were compared. The individual effect of the heel configuration on the tendon tensions, on the wrapping force norms and on joint contact force norms, was made clear.

Statistical analysis

A one-way analysis of variance with repeated measures was used to test the effect of heel configuration (3 levels), per unit body mass, on tendon tensions, on wrapping force norms and on joint contact force norms. In all cases, α was set to 0.05 and statistical significance was accepted for P<0.05; *post hoc* testing of the means was performed using the Bonferroni correction (OriginPro 8)[7].

TABLE 1: Parameters for the distal limb model

Tendon	Element	Segment	Radius (mm)	z%	x%
SDF	Fixed-pulley	Metacarpus	40.1	3.4	7.2
	Variable-pulley	Digit	$d_{SDF}(\theta)$	0	0
	Insertion	Digit	–	74.5	–13.9
SL	Origin	Metacarpus	–	21.6	0.0
	Fixed-pulley	Digit	28.3	0.0	0.0
	Insertion	Digit	–	74.5	–13.9
DDF	Fixed-pulley	Metacarpus	40.1	3.4	7.2
	Variable-pulley	Digit	$d_{DDF}(\theta)$	0	0
	Fixed-pulley	Hoof	22	5	–13.1
	Insertion	Hoof	–	42.5	–17.1

The z axis (directed from the proximal joint toward the distal joint) and *x* axis (directed cranially) values define either coordinate of the origin, insertion and centres of the pulleys in segment-based coordinate system according to Meershoek *et al.* (2001). Values are given as percentage of their respective segment lengths. Fixed-pulley radii are given in mm and variable-pulley radii $d_{SDF}(\theta)$ and $d_{DDF}(\theta)$ are calculated using the fetlock joint angle (θ)-radius pulley variation relationship: $\Delta d_{DDF}(\theta) = -0.24923 \times \theta^1 + 0.00139 \times \theta^2$ ($R^2 = 0.89867$) for the DDF tendon and $\Delta d_{SDF}(\theta) = -0.21494 \times \theta^1 + 0.0012 \times \theta^2$ ($R^2 = 0.91504$) for the SDF tendon.

Results

The parameters for the distal limb model are presented in Table 1. The procedure was executed with a stance duration of 333 ms, which represents 40% of the stride duration, at an average velocity of 4 m/s. The net joint moment, tendon tensions, WF components at the sesamoid bones and the joint contact force components are presented before application of heel wedge in Figure 4. The sensitivity analysis to heel configuration changes is presented in Figure 5.

Net joint moments and tendon tensions

During most of the stance phase, the net joint moments were negative on the palmar side of each joint. These were flexor moments. In the coffin joint the tension of the DDF tendon peaked at 10 ± 1.3 N/kg or 1.02 bwt. In the fetlock joint, the tensions of the SDF tendon and the SL, respectively, peaked at 9 ± 1.5 N/kg or 0.9 bwt and 26 ± 1.6 N/kg or 2.6 bwt.

Wrapping forces and joint contact forces

In the coffin joint the WF exerted by the distal sesamoid bone on the middle phalanx exhibited a peak norm of 13.65 ± 2.6 N/kg or 1.4 bwt. The CF norm exhibited a peak of 24.25 ± 2.7 N/kg or 2.45

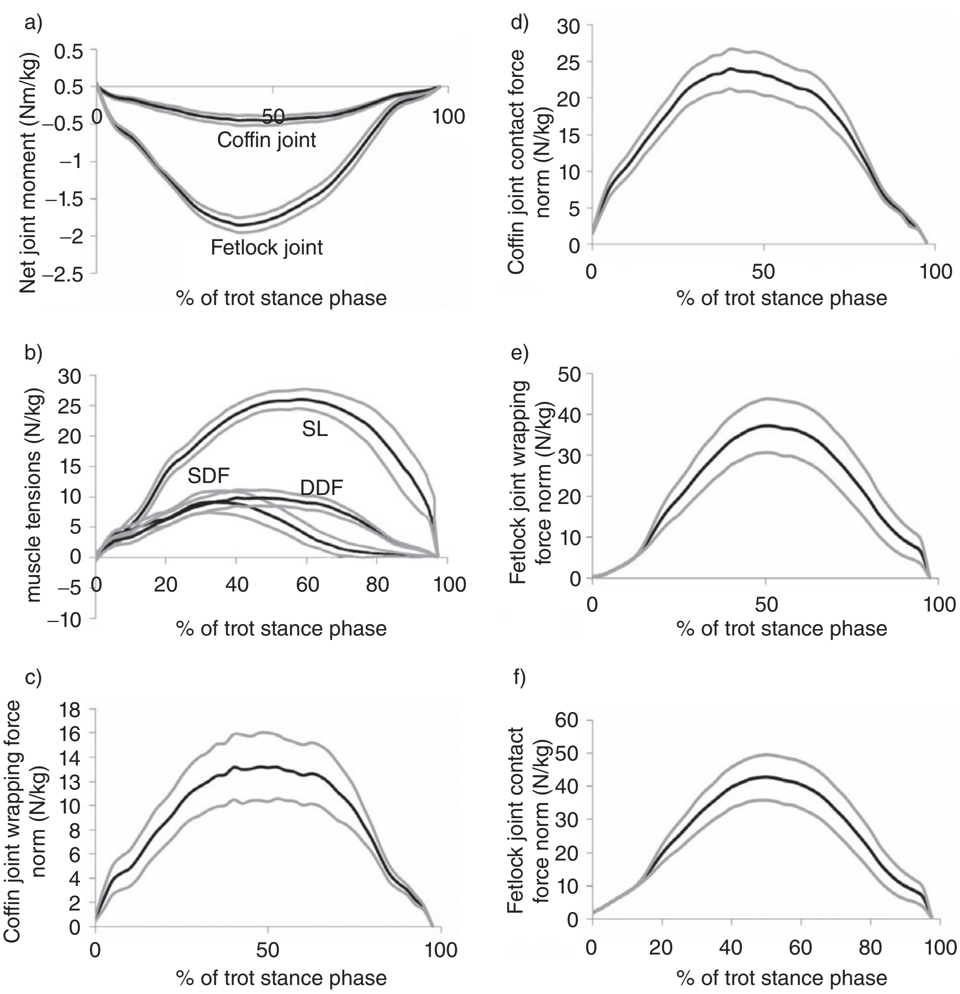

Fig 4: Net joint moment (a), tendon tensions (b), wrapping force norms (c, e), joint contact force norms (d, f) profiles of the coffin and fetlock joints during stance phase of the trot. Values represent the ensemble average for 4 horses ± 1 s.d.

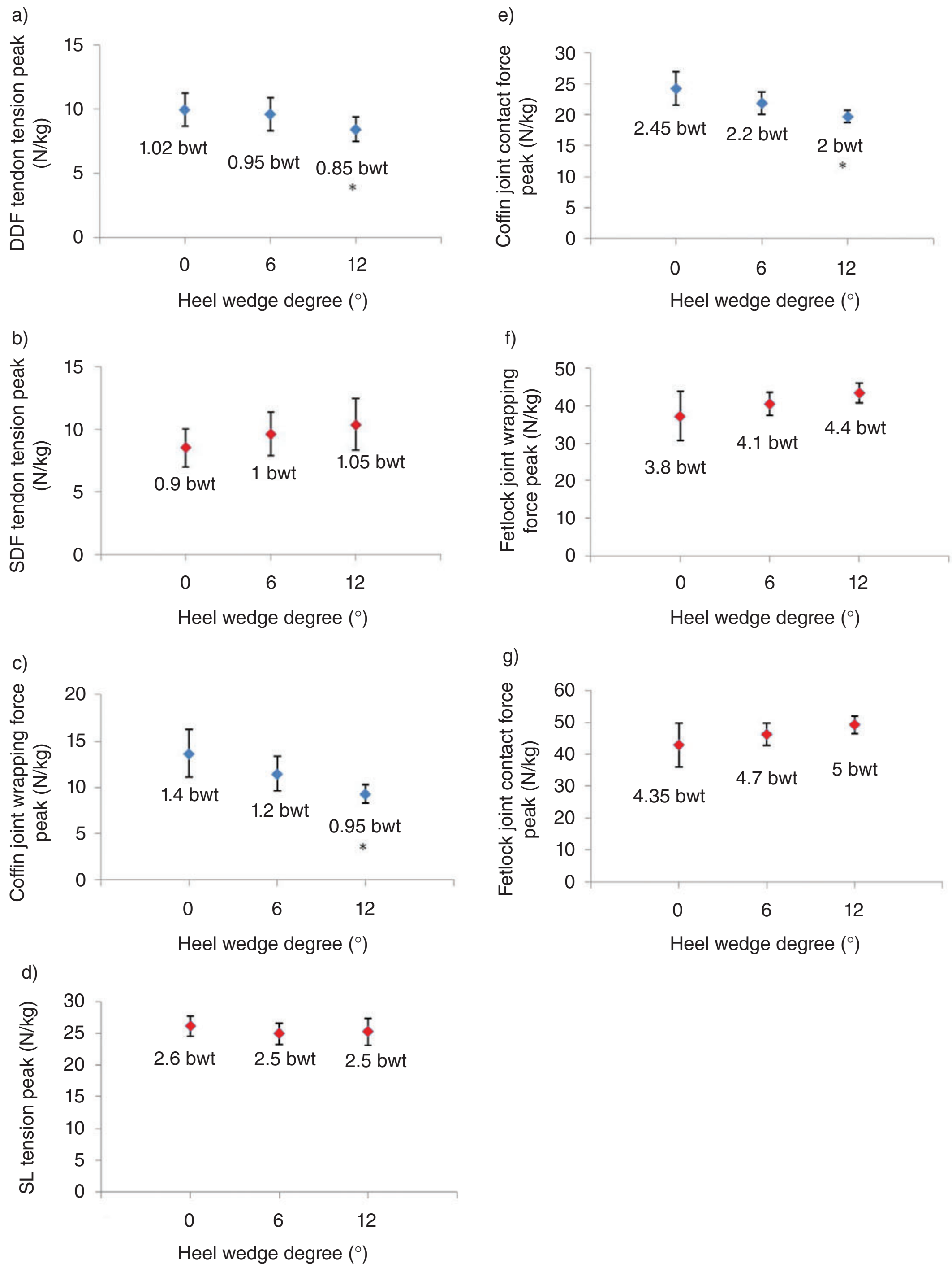

*Fig 5: Sensitivity analysis: effects of the heel wedge configuration on the DDF, the SDF and the SL tension peak (a, b, d); on the wrapping force norm peak (c, f); and on the joint contact force norm peak (e, g) for the coffin and the fetlock joints during the stance phase of the trot. * P<0.05, significant difference for heel configuration.*

bwt. In the fetlock joint, the WF exerted by the proximal sesamoid bone on the metacarpus exhibited a peak norm of 37.2 ± 6.6 N/kg or 3.8 bwt. The CF norm exhibited a peak of 42.9 ± 6.8 N/kg or 4.35 bwt.

Sensitivity analysis

From 0–12° raised: whereas the peak tension of the DDF tendon decreased significantly ($P<0.05$) (1.02 ± 0.13 bwt; 0.95 ± 0.13 bwt; 0.85 ± 0.09 bwt) and the peak tensions of the SDF tendon (0.9 ± 0.15 bwt; 1 ± 0.17 bwt; 1.05 ± 0.21 bwt) and SL (2.6 ± 0.15 bwt; 2.5 ± 0.15 bwt; 2.5 ± 0.2 bwt), respectively, increased and decreased but not significantly, for the coffin joint the peak WF (1.4 ± 0.25 bwt; 1.2 ± 0.2 bwt; 0.95 ± 0.1 bwt) and the peak CF (2.45 ± 0.25 bwt; 2.2 ± 0.2 bwt; 2 ± 0.1 bwt) decreased significantly ($P<0.05$). For the fetlock joint, peak WF (3.8 ± 0.7 bwt; 4.1 ± 0.3 bwt; 4.4 ± 0.25 bwt) and peak CF (4.35 ± 0.7 bwt; 4.7 ± 0.35 bwt; 5 ± 0.3 bwt) increased, but not significantly.

Discussion

The present study offers a new fetlock angle-radius pulley variation relationship at the fetlock joint to model the tendon moment arms, validated experimentally by means of direct measurements. Moreover, the present study brings supplementary data regarding WF and CF components during movement and regarding the effect of heel configuration on joint kinetics. Nevertheless, this procedure had several limitations. The 2D model only considers force components into a sagittal plane. Consequently, the calculation of the oblique force norm may be affected. Additionally, this procedure assumes a perfect frontal symmetry whereas frontal anatomical asymmetry, such as segmental deviation or angular rotation, may influence the CF distribution. Moreover, despite its stiffness, Equi Boot equipment has mechanical properties different to those of the ground (i.e. young modulus). Indeed, our results could be underestimated due to a damping effect of the boot. Finally, like many studies, the procedure makes the assumption that the proximal and middle phalanges can be considered as a single rigid segment. It has previously been shown that the proximal interphalangeal joint (pastern joint) undergoes slight flexion (~3.6°) and then extension (~14.3°) during the stance phase of the trot on treadmill (Chateau *et al*. 2006). Therefore, the calculations of variations in the fetlock and coffin joints angles could be overestimated.

During most of the duration of the stance, the net joint moment was found to be on the palmar side of all the studied joints. These results are in concordance with previous studies of dynamic equine gait analysis (Clayton *et al*. 1998; Dutto *et al*. 2006).

Considering the tendon moment arms, Brown *et al*. (2003) suggested that muscle moment arms in the equine fetlock cannot be modelled as fixed-radius pulleys. In the present study, the tendon moment arms at the fetlock were modelled as variable-radius pulleys and determined using an experimentally validated fetlock angle-radius pulley relationship. Nevertheless, the recursively calculated tendon tension patterns were similar to those presented by Meershoek and Lanovaz (2001) and different to those presented by Merrit *et al*. (2008) building on the work of Brown *et al*. (2003). The differences may be accounted for by the substantially different methods used to calculate tendon tensions. Indeed, the rest length of SL was unknown in the study by Merritt *et al*. (2008), whereas in the present study it was approximated using the method described by Meershoek and Lanovaz (2001). Variations in the SL rest length would cause changes in the SL and SDF tensions.

In previous studies, a link has been postulated between the WF and the CF in the equine distal limb (Willemen *et al*. 1999; Wilson *et al*. 2001; Eliashar *et al*. 2004). The results of the present study are in accordance with this and the work of Merritt *et al*. (2008) which suggested that the magnitudes of the forces exerted due to tendon wrapping contribute substantially to the CF.

In the present study, sensitivity analysis showed that with 0–12° heel wedges, peak tension of the DDF tendon was significantly lower and the peak tension of the SDF was higher but not significantly so. These findings are in accordance with the work of Meershoek *et al*. (2002). Moreover, with heel wedges of 0–12°, the WF and the CF significantly decreased for the coffin joint. This result is not surprising because the coffin joint WF and CF depend substantially on the DDF tendon tension. This confirms the use of heel wedges to reduce loading of the DDF tendon and to reduce the WF exerted on the navicular bone (Riemersma *et al*. 1996; Willemen *et al*. 1999). Nevertheless, we must be prudent concerning the use of heel wedges to reduce coffin joint CF. In the present study, the CF was found to decrease after the addition of a heel wedge due to a decrease in DDF tension and in the WF. However, a previous study found an increase in intra-articular pressure after the addition of a heel wedge due to flexion of the distal interphalangeal joint (coffin joint) (Viitanen *et al*. 2003). These 2 contradictory results show that for the same joint after an orthopaedic treatment (i.e. heel wedge), a cancelled constraint (i.e. tendon tension) may be replaced by another constraint (i.e. compressive flexion). Moreover, our sensitivity analysis showed that with heel wedges of 0–12°, the WF and the CF increased for the fetlock joint. This suggests that coffin and fetlock joint loading are strongly connected and the use of orthopaedic shoeing influences both coffin and fetlock joints. Secondary tendinitis of SDF tendon or fetlock joint disorder after heel wedge application may be explained by these last results. Several kinematic studies have described the effect on upper joints of wedges applied to the limb. Indeed, both Chateau *et al*. (2006) and Peham *et al*. (2006) showed that the use of heel wedges modifies the angle variation of the coffin, pastern and the fetlock joints. Additionally, Back *et al*. (2003) demonstrated some indirect effects on forelimb kinematics of wedges applied to the hindlimb. However, it has also previously been shown that some acute effects of the application of wedges would become nonsignificant over a longer period of post test recordings (Firth *et al*. 1988). Future research studying the chronic effects of the use of heel wedges should prove that employing these aids to reduce loading of the coffin joint may in fact increase loading of the fetlock joint.

Conclusions

Joint contact force components in the equine digit were calculated using a 2D model derived from kinetic and kinematic data. A sensitivity analysis made clear the acute effect of heel configuration changes on joint contact force components. Our results suggest that the use of a heel wedge to reduce the loading of the coffin joint components may increase the loading of the fetlock joint components. The present study could be extended, over a longer period of post test recordings, to a large sample size in order to confirm the effect of heel wedges on the fetlock joint and its suspensor apparatus.

Conflict of interest

None of the authors of this paper has a financial or personal relationship with other people or organisations that could inappropriately influence or bias the content of the paper.

Manufacturers' addresses

[1]Kerckhaert, Vogelwaarde, The Netherlands.
[2]Graber AG Company, Fahrwangen, Switzerland.
[3]BTS Bioengineering, Brescia, Italy.
[4]Tekscan, Inc., South Boston, Virginia, USA.
[5]Easycare Inc., Tucson, Arizona, USA.
[6]Gierth, Riesa, Germany.
[7]OriginLab, Northampton, Massachusetts, USA.

References

Back, W., Remmen, J.L., Knaap, J. and de Koning, J.J. (2003) Effect of lateral heel wedges on sagittal and transverse plane kinematics of trotting Shetland ponies and the influence of feeding and training regimes. *Equine vet. J.* **35**, 606-612.

Brown, N.A., Pandy, M.G., Buford, W.L., Kawcak, C.E. and McIlwraith, C.W. (2003) Moment arms about the carpal and metacarpophalangeal joints for flexor and extensor muscles in equine forelimbs. *Am. J. vet. Res.* **64**, 351-357.

Buchner, H.H., Savelberg, H.H., Schamhardt, H.C. and Barneveld, A. (1997) Inertial properties of Dutch Warmblood horses. *J. Biomech.* **30**, 653-658.

Caudron, I. (1997) *Approche Orthopédique des Affections Ostéo-articulaires Dégénératives de l'Extrémité Digitale du Cheval. Prévention et Traitement*. PhD Thesis, Liège University.

Chateau, H., Degueurce, C. and Denoix, J.M. (2006) Three-dimensional kinematics of the distal forelimb in horses trotting on a treadmill and effects of elevation of heel and toe. *Equine vet. J.* **38**, 164-169.

Clayton, H.M., Lanovaz, J.L., Schamhardt, H.C., Willemen, M.A. and Colborne, G.R. (1998) Net joint moments and powers in the equine forelimb during the stance phase of the trot. *Equine vet. J.* **30**, 384-389.

Dutto, D.J., Hoyt, D.F., Clayton, H.M., Cogger, E.A. and Wickler, S.J. (2006) Joint work and power for both the forelimb and hindlimb during trotting in the horse. *J. expt. Biol.* **209**, 3990-3999.

Eliashar, E., McGuigan, M.P. and Wilson, A.M. (2004) Relationship of foot conformation and force applied to the navicular bone of sound horses at the trot. *Equine vet. J.* **36**, 431-435.

Firth, E.C., Schamhardt, H.C. and Hartman, W. (1988) Measurements of bone strain in foals with altered foot balance. *Am. J. vet. Res.* **49**, 261-265.

Meershoek, L.S. and Lanovaz, J.L. (2001) Sensitivity analysis and application to trotting of a noninvasive method to calculate flexor tendon forces in the equine forelimb. *Am. J. vet. Res.* **62**, 1594-1598.

Meershoek, L.S., Bogert, A.J. and Schamhardt, H.C. (2001) Model formulation and determination of in vitro parameters of a noninvasive method to calculate flexor tendon forces in the equine forelimb. *Am. J. vet. Res.* **62**, 1585-1593.

Meershoek, L.S., Lanovaz, J.L., Schamhardt, H.C. and Clayton, H.M. (2002) Calculated forelimb flexor tendon forces in horses with experimentally induced superficial digital flexor tendinitis and the effects of application of heel wedges. *Am. J. vet. Res.* **63**, 432-437.

Merkens, H.W., Schamhardt, H.C., Van Osch, G.J. and Van den Bogert, A.J. (1993) Ground reaction force patterns of Dutch Warmblood horses at normal trot. *Equine vet. J.* **25**, 134-137.

Merritt, J.S., Davies, H.M., Burvill, C. and Pandy, M.G. (2008) Influence of muscle-tendon wrapping on calculations of joint reaction forces in the equine distal forelimb. *J. Biomed. Biotechnol.* **2008**, 165730.

Peham, C., Girtler, D., Kicker, C. and Licka, T. (2006) Raising heels of hind hooves changes the equine coffin, fetlock and hock joint angle: a kinematic evaluation on the treadmill at walk and trot. *Equine vet. J., Suppl.* **36**, 427-430.

Radin, E.L. (1983) The effects of repetitive loading on cartilage. Advice to athletes to protect their joints. *Acta Orthop. Belg.* **49**, 225-232.

Radin, E.L., Paul, I.L. and Rose, R.M. (1972) Role of mechanical factors in pathogenesis of primary osteoarthritis. *Lancet* **1**, 519-522.

Riemersma, D.J., Bogert, A.J., Jansen, M.O. and Schamhardt, H.C. (1996) Influence of shoeing on ground reaction forces and tendon strains in the forelimbs of ponies. *Equine vet. J.* **28**, 126-132.

Sasimontonkul, S., Bay, B.K. and Pavol, M.J. (2007) Bone contact forces on the distal tibia during the stance phase of running. *J. Biomech.* **40**, 3503-3509.

Viitanen, M.J., Wilson, A.M., McGuigan, H.R., Rogers, K.D. and May, S.A. (2003) Effect of foot balance on the intra-articular pressure in the distal interphalangeal joint in vitro. *Equine vet. J.* **35**, 184-189.

Willemen, M.A., Savelberg, H.H. and Barneveld, A. (1999) The effect of orthopaedic shoeing on the force exerted by the deep digital flexor tendon on the navicular bone in horses. *Equine vet. J.* **31**, 25-30.

Wilson, A.M., McGuigan, M.P., Fouracre, L. and MacMahon, L. (2001) The force and contact stress on the navicular bone during trot locomotion in sound horses and horses with navicular disease. *Equine vet. J.* **33**, 159-165.